Phytochemistry 192 (2021) 112957

Contents lists available at ScienceDirect

Phytochemistry

journal homepage: www.elsevier.com/locate/phytochem

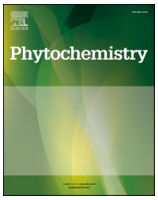

Hygroline derivatives from *Schizanthus tricolor* and their anti-trypanosomatid and antiplasmodial activities

Sylvian Cretton [a,b,*], Grégory Genta-Jouve [c], Marcel Kaiser [d,e], Pascal Mäser [d,e], Orlando Muñoz [f], Thomas Bürgi [g], Muriel Cuendet [a,b], Philippe Christen [a,b]

[a] School of Pharmaceutical Sciences, University of Geneva, 1211, Geneva, 4, Switzerland
[b] Institute of Pharmaceutical Sciences of Western Switzerland, University of Geneva, 1211, Geneva, 4, Switzerland
[c] Laboratoire Ecologie, Evolution, Interactions des Systèmes Amazoniens (LEEISA), USR 3456, Université De Guyane, CNRS Guyane, 97300, Cayenne, French Guyana, France
[d] Swiss Tropical and Public Health Institute, 4002, Basel, Switzerland
[e] University of Basel, 4003, Basel, Switzerland
[f] Departamento de Química, Facultad de Ciencias, Universidad de Chile, Casilla 653, Santiago, Chile
[g] Department of Physical Chemistry, University of Geneva, 1211, Geneva, 4, Switzerland

ARTICLE INFO

Keywords:
Schizanthus tricolor
Solanaceae
Hygroline derivatives
Pyrrolidine alkaloids
Antiparasitic activity

ABSTRACT

Chemical investigation of the alkaloid extract of the aerial parts of *Schizanthus tricolor* led to the targeted isolation of 26 hygroline derivatives of which 20 were fully characterized. They have not yet been described in the literature and their structures were established by 1D and 2D NMR, UV and IR spectroscopy, and HRESIMS. The configuration was determined by Gauge-Independent Atomic Orbital NMR chemical shift calculations supported by the advanced statistical method DP4 plus, vibrational circular dichroism, and measurement of optical rotation. Their anti-trypanosomatid, antiplasmodial and cytotoxic activities were measured. Several compounds exhibited low micromolar activity against *Plasmodium falciparum*. None of the identified molecules was cytotoxic.

1. Introduction

The genus *Schizanthus* Ruiz & Pav. from the Solanaceae family comprises 12 species and are commonly known as little bird or little butterfly. This genus is primarily native to Chile and the species grow in a large diversity of habitats, from the desert to the coast, as well as from the high Andes to areas cleared of forest in the southern region (Pérez et al., 2006). The genus is characterized by numerous tropane alkaloids. Most of them are ester derivatives from angelic, senecioic, tiglic, itaconic, mesaconic, citraconic or cinnamic acid, which generates numerous positional and configurational isomers. To date over 50 alkaloids have been isolated and characterized from this genus. However, among them only seven pyrrolidine derivatives were described, namely hygrine, hygrolines, cuscohygrines, 4-hydroxyphenylpropanoylhygroline, and 1-methyl-2-(1-methyl-2-pyrrolidinyl)-ethyl-6-deoxy-3-*O*-angeloyl-*α*-galactopyranoside (Christen et al., 2020). Pyrrolidine derivatives are a source of pharmacologically active lead compounds (Islam and Mubarak, 2020) and the object of recent synthesis due to "their intriguing biological activities, hallucinogenic characteristics and their utility as pharmacological probes" (Bhat and Tilve, 2011). Therefore, the aim of this study was to investigate the diversity of pyrrolidine derivatives in the species *Schizanthus tricolor* Grau & Gronbach (Solanaceae) which is known to be particularly rich in alkaloids. In addition, as part of our ongoing research of undescribed antiprotozoal molecules (Cretton et al., 2010, 2014a, 2014b, 2020), the antiparasitic activity of the isolated hygroline derivatives was evaluated against *Trypanosoma brucei rhodesiense* (*T.b. rhodesiense*), *Trypanosoma cruzi* (*T. cruzi*), *Leishmania donovani* (*L. donovani*), and *Plasmodium falciparum* (*P. falciparum*).

2. Results and discussion

The alkaloid extract from the aerial parts of *S. tricolor* was analyzed by LC-HRMS/MS in positive mode. The MS/MS fragment at *m/z* 144.1390, characteristic of the hygroline moiety was used as a marker to identify putative pyrrolidine alkaloids (see supporting information). An early eluting broad peak displaying ion at *m/z* 290 $[M + H]^+$, followed

* Corresponding author. School of Pharmaceutical Sciences, University of Geneva, 1211, Geneva, 4, Switzerland.
E-mail address: sylvian.cretton@unige.ch (S. Cretton).

https://doi.org/10.1016/j.phytochem.2021.112957
Received 22 July 2021; Received in revised form 13 September 2021; Accepted 15 September 2021
Available online 23 September 2021

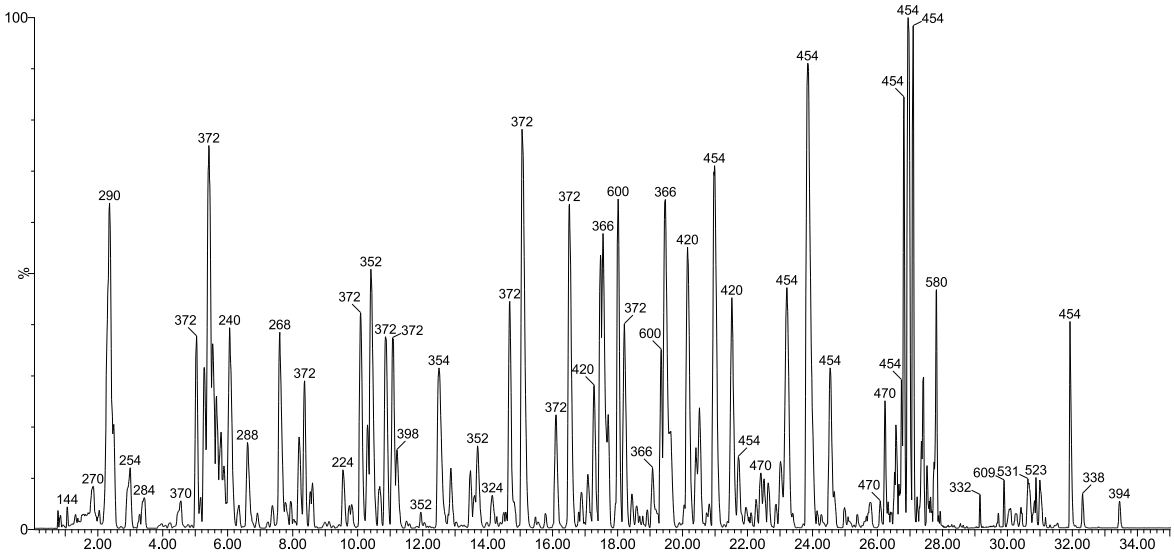

Fig. 1. LC-HRMS chromatogram of the alkaloid fraction of *S. tricolor* (for sake of clarity *m/z* values are shown without decimal).

by 17 peaks at *m/z* 372 $[M + H]^+$, 6 peaks at *m/z* 600 $[M + H]^+$, 4 peaks at *m/z* 420 $[M + H]^+$, and 18 peaks at *m/z* 454 $[M + H]^+$ were identified as putative pyrrolidine derivatives (Fig. 1). To isolate the targeted hygroline derivatives, the alkaloid extract was fractionated using flash chromatography. Further purification of the fractions was carried out by semi-preparative HPLC and afforded 20 fully characterized undescribed compounds, **1**–**20** (Fig. 2).

Compound **1** was obtained as a pale yellow oil, and its molecular formula $C_{14}H_{26}NO_5$ was established by HRESIMS data (*m/z* 290.1979 $[M + H]^+$, calcd for $C_{14}H_{27}NO_5$, 290.1962). The IR spectrum showed absorption bands attributable to hydroxy (3255 cm^{-1}) and amine (1591 cm^{-1}) groups. Analysis of NMR data (Table 1), and comparison with the literature (Muñoz et al., 1994) indicated the presence of a deoxy hexose sugar unit with proton signals at δ_H 4.72, 3.49, 3.44, 3.47, 3.86, 1.06 (H-1 to H-6, respectively) and their corresponding carbon signals at δ_C 100.1, 68.0, 70.1, 71.5, 66.4 and 16.5. The configuration of the sugar unit was determined by VCD. A positive sign of the intense glycoside band around 1160 cm^{-1} was observed on the VCD spectrum of **1** (Fig. 3) and indicates an axial glycosidic linkage in C-1, with the $^1C_4$ conformation (Taniguchi and Monde, 2007a,b). Therefore, the proton H-1 is oriented in equatorial position and the small coupling constant between H-1 and H-2 ($J = 3.6$ Hz) indicated that H-2 is in axial position (Fig. 4). Likewise, the coupling constants between H-2 and H-3 ($J = 10.0$ Hz) imposed an axial orientation for H-3, and an equatorial orientation for H-4 ($J = 3.4$ Hz). Due to an overlapping of the signals of H-2 to H-4 in DMSO-d_6, a second measurement was performed in CD_3OD, which made it possible to confirm the spin system (see supporting information, Table S3). From these data, a β-6-deoxy-L-galactose (also named β-L-fucose) unit was identified. A hygroline moiety was deduced from eight carbon signals corresponding to two methine C-2′ and C-7′ (δ_C 64.3 and 73.5, respectively) each linked to a heteroatom (N and O, respectively), four methylenes C-3′ to C-6′ (δ_C 28.4, 21.1, 55.8 and 36.7, respectively), and two methyl groups C-8′ and C-9′ (δ_C 21.8 and 39.2, respectively). A key HMBC correlation between H-7′ at δ_H 3.78 (m, 1H) and C-1, as well as a ROE interaction between H-7′ and H-1 allowed to connect the hygroline moiety to the anomeric carbon (C-1) of the fucose unit (Fig. 4). Unfortunately, the high flexibility of this molecule impeded the determination of the absolute configuration by comparison of the calculated and experimental VCD spectra. Therefore, the relative configurations at C-2′ and C-7′ were assigned by calculation of the Smith and Goodman DP4 probability (Smith and Goodman, 2010). Comparison of the experimental and theoretical chemical shifts indicated a 2′*S**/7′*S** configuration with 85.9% probability (see supporting information). To confirm this result, the absolute configuration of the hygroline moiety was determined by an acidic hydrolysis of **1** followed by the optical rotation measurement of the hygroline moiety $[\alpha]_D^{22}$ – 48.2 (*c* 0.05, EtOH). A comparison with the literature $[\alpha]_D^{24}$ - 46.9 (*c* 1.00, EtOH) (Liniger et al., 2013) corroborated the 2′*S*/7′*S* configuration. Likewise, the optical rotation of the resulting sugar was compared to that of L-fucose and confirmed the identity of the 6-deoxy hexose. Compound **1** was thus identified as 1(*S*)-methyl-2-(1-methyl-2(*S*)-pyrrolidinyl)ethyl 6-deoxy-β-galactopyranoside, and named schizanthoside A1.

Compound **2** shares the same HRESIMS protonated molecule $[M + H]^+$ at *m/z* 290.1979 (calcd for $C_{14}H_{27}NO_5$, 290.1962) than **1,** and consequently both compounds are isomers. IR and NMR data are also very similar. To distinguish them, a DP4 calculation was carried out and established a 2′*R**/7′*S** configuration at 81.1% for **2**. An acid hydrolysis of **2** followed by the measurement of the optical rotation of the hygroline moiety $[\alpha]_D^{22}$ + 98.2 (*c* 0.05, EtOH), and comparison with the literature (Liniger et al., 2013) confirmed the presence of a (+)-pseudohygroline moiety for **2**. L-fucose was also confirmed by comparison of its optical rotation with a standard sample. Compound **2** was thus identified as 1 (*S*)-methyl-2-(1-methyl-2(*R*)-pyrrolidinyl)ethyl 6-deoxy-β-galactopyranoside, and named schizanthoside A2.

The HRMS, IR and NMR data of compound **3** are very similar to those of **1** and **2**. Nevertheless, a noticeable difference lies in the multiplicity and the constant coupling of H-4 at δ_H 2.77 (t, $J = 9.2$ Hz, 1H), indicating that H-4 is axially oriented and characteristic of a 6-deoxy-glucose ring (Fig. 4). According to the DP4 probability, a 2′*R**/7′*S** configuration was established (82.8%). Therefore, compound **3** was identified as 1(*S*)-methyl-2-(1-methyl-2(*R*)-pyrrolidinyl)ethyl 6-deoxy-β-glucopyranoside, and named schizanthoside A3.

The molecular formula $C_{19}H_{33}O_6$ of **4** was established by HRESIMS from the protonated molecule $[M + H]^+$ at *m/z* 372.2385 (calcd for $C_{19}H_{34}NO_6$, 372.2381). MS/MS fragment at *m/z* 83.0499 (see supporting information) suggested the presence of a monocarboxylic isomeric C_5 acid, namely angelic, senecioic or tiglic acids that are known to be present in the genus *Schizanthus* (Christen et al., 2020). Analysis of ^{1}H-NMR data revealed signals of two methyl groups at δ_H 1.97 (dq, $J =$ 7.3 and 1.6 Hz, H-4″) and at δ_H 1.86 (t, $J = 1.6$ Hz, H-5″), and a vinylic proton at δ_H 6.18 (qd, $J = 7.3$ and 1.6 Hz, H-3″). On the DEPTQ spectrum, a carbonyl signal at δ_C 167.1 (C-1″), two sp^2 carbon signals at δ_C 127.3 (C-2″) and 138.7 (C-3″), and two methyl signals at δ_C 15.8 (C-4″) and 20.5 (C-5″) were observed. 2D experiments (COSY and HMBC)

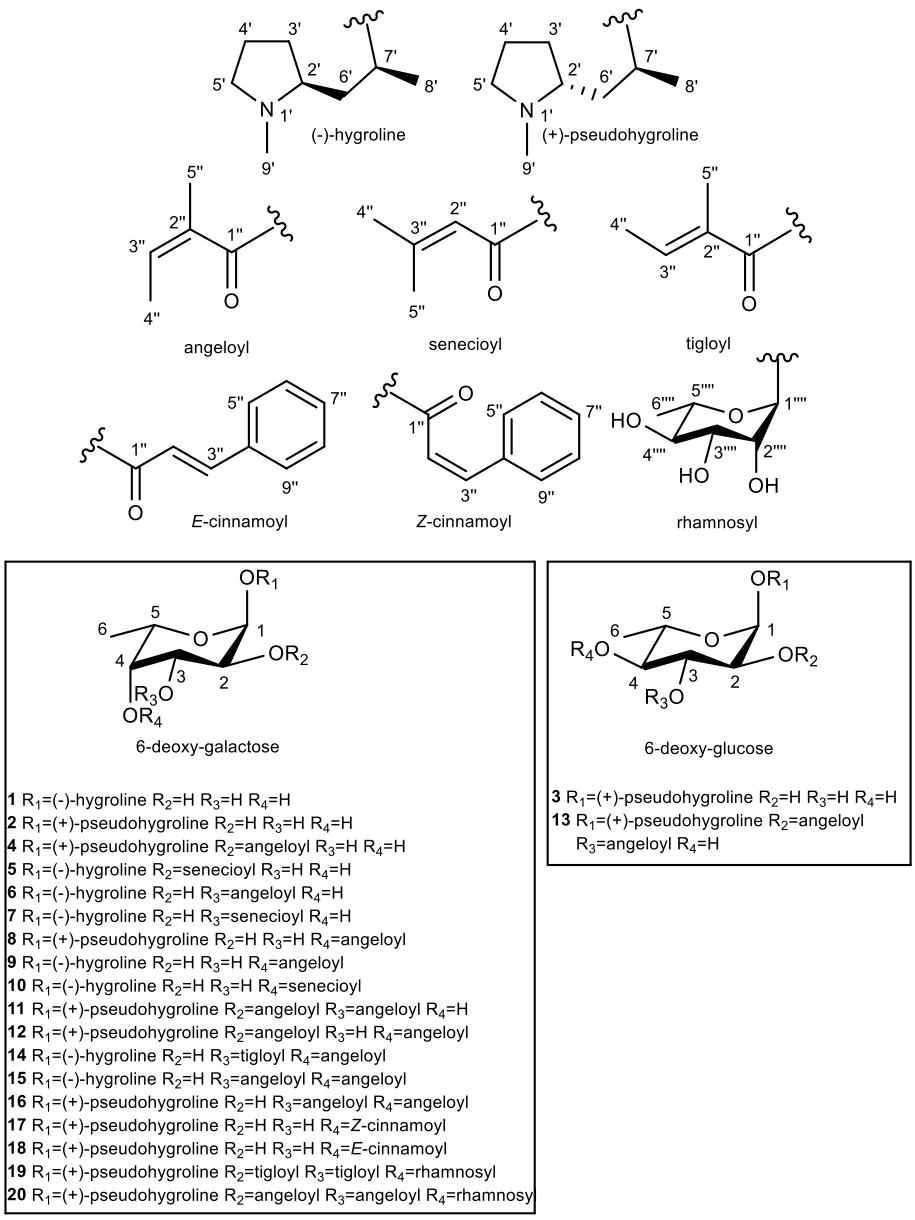

Fig. 2. Chemical structures of compounds **1**–**20**.

allowed to interconnect the different elements, and to identify angelic acid as esterifying acid (De la Fuente et al., 1988). A deshielding of proton H-2 in the fucose ring located the esterification of angelic acid in C-2 (Muñoz et al., 1994). According to the DP4 probability, a 2′*R**/7′*S** configuration was established (93.2%) and the compound was characterized as 1(*S*)-methyl-2-(1-methyl-2(*R*)-pyrrolidinyl)ethyl 6-deoxy-2--*O*-angeloyl-*β*-galactopyranoside and named schizanthoside B1.

Compound **5** differs from compound **4** by the nature of the C_5 acid esterifying the fucose skeleton in C-2. Indeed, in the ^{1}H-NMR spectrum a signal corresponding to the vinylic proton H-2″ at δ_H 5.82 (d, $J = 2.0$ Hz) was observed. The COSY experiment demonstrated that H-2″ correlated with two methyl groups at δ_H 1.96 (d, $J = 2.0$ Hz, H-4″), and at δ_H 2.21 (d, $J = 2.0$ Hz, H-5″). This coupling system and the chemical shifts are characteristic of senecioic acid (De la Fuente et al., 1988). According to the DP4 probability, a 2′*S**/7′*S** configuration was established (79.4%), and **5** was characterized as 1(*S*)-methyl-2-(1-methyl-2(*S*)-pyrrolidinyl) ethyl 6-deoxy-2-*O*-senecioyl-*β*-galactopyranoside, and named schizanthoside B2.

A comparison of the NMR data of **6** with the literature (Muñoz et al., 1994) indicated that **6** was characterized by the following structure 1-methyl-2-(1-methyl-2-pyrrolidinyl)ethyl 6-deoxy-3-*O*-angeloyl-galacto pyranoside. DP4 calculation allowed to attribute a 2′*S**/7′*S** configuration and the alkaloid was identified as 1(*S*)-methyl-2-(1-methyl-2(*S*)-pyrrolidinyl)ethyl 6-deoxy-3-*O*-angeloyl-*β*-galactopyranoside, and named schizanthoside B3. Compound **6** has an optical rotation value of $[\alpha]_D^{22}$ - 71.6 (*c* 0.05, MeOH), which differs from the published data $[\alpha]_D^{20}$ + 14.2 (*c* 1.03, EtOH) indicating a difference in the stereochemistry of the hygroline and/or the sugar moiety. Unfortunately, no data about the stereochemistry was published, and prevents a comparison of the two stereoisomers.

Compound **7** is similar to **6** except that senecioic acid, characterized by H-2″ at δ_H 5.72 and two methyl groups at δ_H 1.88 (H-4″), and at δ_H 2.10 (H-5″), is esterified in C-3 instead of angelic acid for **6**. DP4 calculation allowed to attribute at 80.5% a 2′*S**/7′*S** configuration and **7** was identified as 1(*S*)-methyl-2-(1-methyl-2(*S*)-pyrrolidinyl)ethyl 6-deoxy-3-*O*-senecioyl-*β*-galactopyranoside, and named schizanthoside B4.

Compound **8** is composed of a fucose unit esterified by angelic acid with the characteristic vinylic proton at δ_H 6.10 (qd, $J = 7.2$ and 1.7 Hz,

Table 1
^{1}H and^{13}C NMR data of compounds **1**–**3** (600 and 150 MHz, in DMSO-d_6, δ in ppm).

Position	1 δ_H, (J in Hz)	δ_C, type	2 δ_H, (J in Hz)	δ_C, type	3 δ_H, (J in Hz)	δ_C, type
1	4.72, d (3.6)	100.1, CH	4.65, d (2.8)	100.2, CH	4.64, d (3.9)	99.9, CH
2	3.49, dd (10.0, 3.6)	68.0 CH	3.51, m	68.3, CH	3.17, dd (9.7, 3.9)	72.3, CH
3	3.44, d (10.0, 3.4)	70.1, CH	3.51, m	69.6, CH	3.33, t (9.2)	72.9, CH
4	3.47, d (3.4)	71.5, CH	3.47, brs	71.7, CH	2.77, t (9.2)	75.8, CH
5	3.86, q (6.5)	66.4, CH	3.85, qd (6.6, 1.4)	66.1, CH	3.55, m	67.5, CH
6	1.06, d (6.5)	16.5, CH_3	1.06, d (6.6)	16.5, CH_3	1.09, d (6.3)	17.8, CH_3
2′	2.52, m	64.3, CH	2.42, m	62.5, CH	2.59, m	62.7, CH
3′	1.93, m 1.62, m	28.4, CH_2	1.95, m 1.42, m	30.2, CH_2	2.00, m 1.46, m	29.9, CH_2
4′	1.71, m	21.1, CH_2	1.62, m	21.4, CH_2	1.66, m	21.3, CH_2
5′	3.09, brs 2.33, brs	55.8, CH_2	2.96, ddd (9.5, 7.4, 3.4) 2.15, d (9.5)	56.4, CH_2	3.04, m 2.26, d (9.2)	56.0, CH_2
6′	1.73, m 1.62, m	36.7, CH_2	1.83, ddd (13.2, 9.0, 3.9) 1.22, m	40.6, CH_2	1.86, ddd (13.4, 9.4, 3.9) 1.30, td (9.4, 4.6)	40.0, CH_2
7′	3.78, m	73.5, CH	3.61, ddd (9.4, 6.2, 3.4)	74.1, CH	3.63, m	74.5, CH
8′	1.17, d (6.0)	21.8, CH_3	1.17, d (6.2)	22.5, CH_3	1.18, d (6.2)	22.5, CH_3
9′	2.38, s	39.2, CH_3	2.23, s	39.9, CH_3	2.30, s	39.5, CH_3

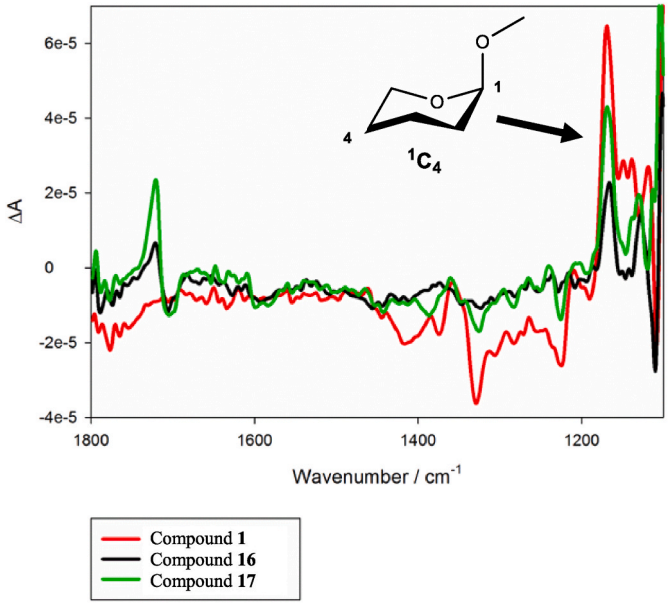

Fig. 3. Experimental VCD spectra of compounds **1**, **16** and **17**.

H-3″), and two methyl groups at δ_H 1.93 (dq, J = 7.2 and 1.7 Hz, H-4″), and at δ_H 1.86 (t, J = 1.7 Hz, H-5″). The esterification site was located in C-4 by the deshielding of proton H-4 at δ_H 5.13 (d, J = 3.2 Hz), and a HMBC correlation between H-4 and C-1″ at δ_C 167.0. DP4 calculation allowed to attribute a 2′*R**/7′*S** configuration and the compound was identified as 1(*S*)-methyl-2-(1-methyl-2(*R*)-pyrrolidinyl)ethyl 6-deoxy-4-*O*-angeloyl-*β*-galactopyranoside, and named schizanthoside B5.

Compound **9** has the same structure as **8** except that DP4 calculation determined 2′*S**/7′*S** configuration for the hygroline moiety. Therefore, **9** was identified as 1(*S*)-methyl-2-(1-methyl-2(*S*)-pyrrolidinyl)ethyl 6-deoxy-4-*O*-angeloyl-*β*-galactopyranoside, and named schizanthoside B6.

Compound **10** differs from **8** and **9** by the presence of senecioic acid esterified in C-4. The nature of the acid was identified by the proton H-2″ at δ_H 5.72 and two methyl groups at δ_H 1.89 (H-4″), and at δ_H 2.10 (H-5″). DP4 calculation allowed to determine a 2′*S**/7′*S** configuration and **10** was identified as 1(*S*)-methyl-2-(1-methyl-2(*S*)-pyrrolidinyl)ethyl 6-deoxy-4-*O*-senecioyl-*β*-galactopyranoside, and named schizanthoside B7.

The molecular formula $C_{24}H_{39}NO_7$ of compound **11** was deduced from the protonated molecule $[M + H]^+$ at *m/z* 454.2797 (calcd for $C_{24}H_{40}NO_7$, 454.2800). A comparison with the molecular formula of the isomers at *m/z* 372.2385 indicated a difference of C_5H_6O, which could correspond to an additional C_5 acid esterified on the fucose moiety. This assumption was corroborated by the analysis of the ^{1}H-NMR spectrum where two vinylic protons at δ_H 6.19 (1H, qd, J = 7.3 and 1.9 Hz, H-3″) and at δ_H 6.11 (1H, qd, J = 7.2 and 1.5 Hz, H-3‴), and four methyl groups at δ_H 1.87 (6H, m, H-4″ and H-4‴), and at δ_H 1.78 (6H, dt, J = 8.9 and 1.6 Hz, H-5″ and H-5‴) were observed. The chemical shifts are characteristic of two angelic acids and their location on the sugar was determined in C-2 and C-3 by the deshielding of protons H-2 at δ_H 5.10 (1H, dd, J = 11.0 and 3.8 Hz), and H-3 at δ_H 5.19 (1H, dd, J = 11.0 and 3.2 Hz). In addition, HMBC correlations were observed from H-2 to C-1″ at δ_C 166.5 and from H-3 to C-1‴ at δ_C 166.6. DP4 calculation determined a 2′*R**/7′*S** configuration for the hygroline part and **11** was characterized as 1(*S*)-methyl-2-(1-methyl-2(*R*)-pyrrolidinyl)ethyl 6-deoxy-2,3-*O*-diangeloyl-*β*-galactopyranoside, and named schizanthoside C1.

Compound **12** is an isomer of **11** and showed close structural similarities. However, according to NMR data the second angelic acid is esterified in C-4 instead of C-3 in **11**. Indeed, HMBC correlations were observed between H-2 at δ_H 4.76 (1H, dd, J = 10.6 and 3.8 Hz) and C-1″ at δ_C 166.8, and between H-4 at δ_H 5.21 (1H, d, J = 3.6 Hz) and C-1‴ at δ_C 166.9. DP4 calculation determined a 2′*R**/7′*S** configuration for the hygroline part and **12** was characterized as 1(*S*)-methyl-2-(1-methyl-2(*R*)-pyrrolidinyl)ethyl 6-deoxy-2,4-*O*-diangeloyl-*β*-galactopyranoside, and named schizanthoside C2.

The HRMS and spectral data of compound **13** were very similar to those of compound **11**. Nevertheless, an analysis of the coupling constants of the sugar protons pointed out a difference in the multiplicity. The coupling constant of H-4 at δ_H 3.21 (1H, t, J = 9.3 Hz) indicated that H-4 is axially oriented. DP4 calculation determined a 2′*R**/7′*S** configuration for the hygroline moiety and **13** was characterized as 1(*S*)-methyl-2-(1-methyl-2(*R*)-pyrrolidinyl)ethyl 6-deoxy-2,3-*O*-diangeloyl-*β*-glucopyranoside, and named schizanthoside C3.

Compound **14** contrasts from the previous isomers (**11**–**13**) by the presence of tiglic acid revealed by the vinylic proton at δ_H 6.67 (1H, qd, J = 7.2 and 1.8 Hz, H-3″) (De la Fuente et al., 1988). HMBC correlation from H-3 at δ_H 5.06 (1H, dd, J = 10.6 and 3.5 Hz) to C-1″ at δ_C 166.1 allowed to locate tiglic acid in C-3. Likewise, a correlation from H-4 at δ_H 5.24 (1H, d, J = 3.5 Hz) to C-1‴ at δ_C 166.3 positioned angelic acid in C-4. A 2′*S**/7′*S** configuration was determined by DP4 calculation for the hygroline moiety and **14** was characterized as 1(*S*)-methyl-2-(1--methyl-2(*S*)-pyrrolidinyl)ethyl 6-deoxy-3-*O*-tigloyl-4-*O*-angeloyl-*β*-glucopyranoside, and named schizanthoside C4.

Compounds **15** and **16** share the same fucose moiety esterified in C-3 and C-4 by two angelic acids. The sites of esterification were elucidated unambiguously by the deshielding of protons H-3 at δ_H 5.09 (1H, dd, J = 10.6 and 3.5 Hz) for **15** and at δ_H 5.11 (1H, dd, J = 10.5 and 3.5 Hz) for **16**, and by H-4 at δ_H 5.28 (1H, d, J = 3.5 Hz) for **15** and at δ_H 5.26 (1H,

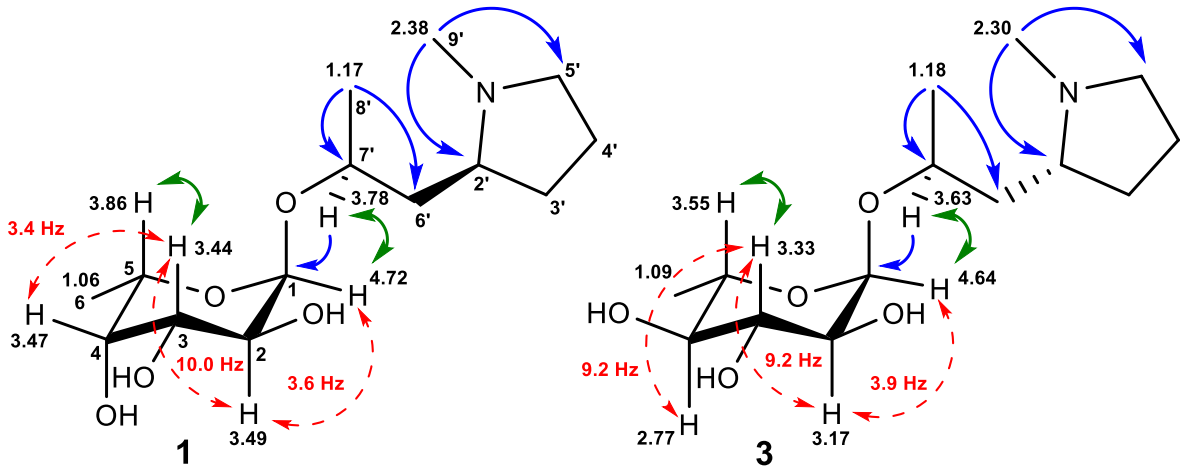

Fig. 4. Key HMBC (blue arrows), ROESY (green arrows) correlations and selected coupling constants (red dashed arrow) of compounds **1** and **3**. (For interpretation of the references to color in this figure legend, the reader is referred to the Web version of this article.)

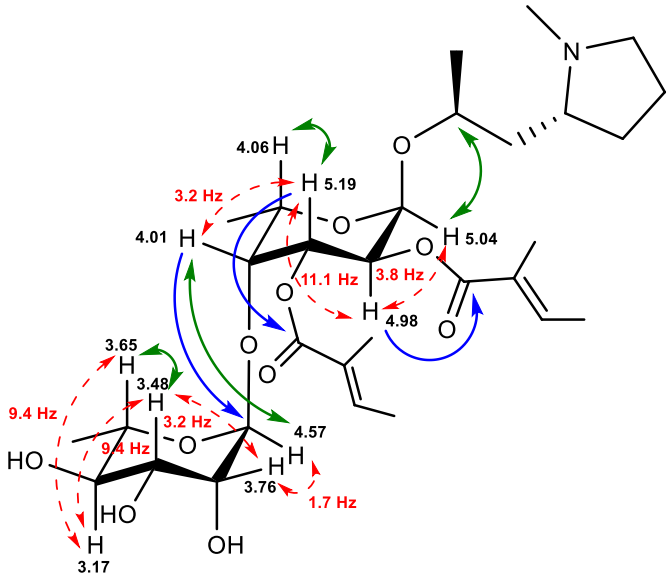

Fig. 5. Key HMBC (blue arrows), ROESY (green arrows) correlations and selected coupling constants (red dashed arrow) of compound **19**. (For interpretation of the references to color in this figure legend, the reader is referred to the Web version of this article.)

dd, $J = 3.5$ and 1.3 Hz) for **16**. For both compounds, HMBC correlations from H-3 to C-1″and H-4 to C-1‴ confirmed the location of the esterified acids on the fucose moiety. However, a 2′*S**/7′*S** configuration for **15** and a 2′*R**/7′*S** for **16** were determined by DP4 calculation. Thus, **15** and **16** were described as 1(*S*)-methyl-2-(1-methyl-2(*S*)-pyrrolidinyl) ethyl 6-deoxy-3,4-*O*-diangeloyl-*β*-galactopyranoside and 1(*S*)-methyl-2-(1-methyl-2(*R*)-pyrrolidinyl)ethyl 6-deoxy-3,4-*O*-diangeloyl-*β*-galactopyranoside, and named schizanthosides C5 and C6, respectively.

Compound **17** exhibited an HRESIMS protonated molecule $[M + H]^+$ at *m/z* 420.2388 (calcd for $C_{23}H_{34}NO_6$, 420.2381), indicating a molecular formula $C_{23}H_{33}NO_6$. NMR data showed the presence of a *cis*-cinnamoyl group characterized by two olefinic methine signals at δ_H 6.06 (1H, d, $J = 12.8$ Hz, H-2″) and at δ_H 7.01 (1H, d, $J = 12.8$ Hz, H-3″), and five aromatic proton signals at δ_H 7.35 (3H, m, H-6″ to H-8″) and δ_H 7.66 (2H, dd, J = 7.4 and 2.2 Hz, H-5″ and H-9″). The coupling constant value $J_{2'',3''}$ of 12.8 Hz indicated a *cis* geometry of the double bond. Key HMBC correlation from proton H-4 at δ_H 5.11 (1H, d, $J = 3.6$ Hz) to C-1″ at δ_C 165.4 allowed to determine the connection of the cinnamoyl moiety to the deoxy galactosyl unit in C-4. A 2′*R**/7′*S** configuration was established by DP4 calculation and the compound was identified as 1(*S*)-methyl-2-(1-methyl-2(*R*)-pyrrolidinyl)ethyl 6-deoxy-4-*O*-(*Z*)-cinnamoyl-*β*-galactopyranoside, and named schizanthoside D1.

Compound **18** shares the same protonated molecule $[M + H]^+$ at *m/z* 420.2388 (calcd for $C_{23}H_{34}NO_6$, 420.2381) as **17**. As for the latter, a cinnamoyl group was characterized by two olefinic methine signals at δ_H 6.66 (1H, d, $J = 16.0$ Hz, H-2″) and δ_H 7.65 (1H, d, $J = 16.0$ Hz, H-3″), and five aromatic proton signals at δ_H 7.43 (3H, m, H-6″ to H-8″) and δ_H 7.74 (2H, m, H-5″ and H-9″). Unlike **17**, the coupling constant value $J_{2'',3''}$ of 16.0 Hz implied a *trans* geometry of the double bond. As for **17**, a key HMBC correlation from proton H-4 at δ_H 5.16 (1H, d, $J = 3.7$ Hz) to C-1″ at δ_C 165.8 allowed to determine the connection of the cinnamoyl moiety to the 6-deoxygalactopyranosyl ring in C-4. A 2′*R**/7′*S** configuration was established by DP4 calculation and the compound was characterized as 1(*S*)-methyl-2-(1-methyl-2(*R*)-pyrrolidinyl)ethyl 6-deoxy-4-*O*-(*E*)-cinnamoyl-*β*-galactopyranoside, and named schizanthoside D2.

The molecular formula of the alkaloid **19** is $C_{30}H_{49}NO_{11}$, and was deduced from the protonated molecule $[M + H]^+$ at *m/z* 600.3386 (calcd for $C_{30}H_{50}NO_{11}$, 600.3379). The analysis of the NMR data showed the presence of a *β*-L-fucose unit esterified with a hygroline moiety in C-1, two tiglic acids in C-2 and C-3, and a rhamnose unit in C-4. The structure of the second sugar unit was inferred from the coupling constant system (1.7 Hz for the anomeric proton, 3.2 Hz between H-2‴″ and H-3‴″, 9.4 Hz between H-3‴″, H-4‴″ and H-5‴″), as well as a ROESY correlation between H-3‴″ and H-5‴″ (Fig. 5). A 2′*R**/7′*S** configuration was determined by DP4 calculation and the compound was identified as 1(*S*)-methyl-2-(1-methyl-2(*R*)-pyrrolidinyl)ethyl 6-deoxy-2,3-*O*-ditigloyl-4-rhamnosyl-*β*-galactopyranoside, and named schizanthoside E1.

Compound **20** is similar to **19** except that two angelic acids are esterified in C-2 and C-3 in the fucose unit instead of two tiglic acids in **19**. A 2′*R**/7′*S** configuration was determined by DP4 calculation and the compound was identified as 1(*S*)-methyl-2-(1-methyl-2(*R*)-pyrrolidinyl)ethyl 6-deoxy-2,3-*O*-diangeloyl-4-rhamnosyl-*β*-galactopyranoside, and named schizanthoside E2.

Six additional isomers at *m/z* 372 were isolated but not fully characterized due to the low amount of the compounds. Indeed, the NMR spectra did not allow to observe all the carbons and protons of the hygroline moiety (see supporting information, Tables 1 and 2), and consequently to determine the stereochemistry. Nevertheless, the nature of the sugar, the C_5 acids and their location on the 6-deoxy-hexose were elucidated without ambiguity. Their structures are depicted in Fig. 6.

The alkaloid extract and seventeen isolated compounds were tested for their in vitro growth inhibition of *T. b. rhodesiense*, *T. cruzi*,

Table 2
^{1}H NMR data of compounds **4**–**10** (600 MHz, in DMSO-d_6 or * CD_3OD, δ in ppm, J in Hz).

Position	4	5*	6	7	8	9	10
1	4.90, d (3.9)	5.08, d (3.7)	4.73, d (3.9)	4.76, d (3.9)	4.79, d (4.0)	4.93, d (3.8)	4.77, d (3.8)
2	4.76, dd (10.6, 3.9)	4.91, dd (10.5, 3.8)	3.84, dd (10.7, 3.9)	3.70, dd (10.9, 3.2)	3.55, dd (10.3, 3.7)	3.56, dd (10.0, 4.0)	3.44, m
3	3.81, dd (10.5, 3.3)	3.92, dd (10.5, 3.4)	4.83, dd (10.7, 3.2)	4.80, dd (10.9, 3.2)	3.77, dd (10.3, 3.7)	3.70, dd (10.0, 3.3)	3.67, dd (10.1, 3.6)
4	3.56, d (3.4)	3.73, d (3.2)	3.69, d (3.2)	3.60, s	5.13, d (3.2)	5.14, d (3.3)	5.04, d (3.6)
5	3.92, q (6.5)	4.07, q (6.6)	3.94, q (6.5)	3.94, q (6.6)	4.10, q (6.5)	4.12, q (6.6)	4.06, q (6.7)
6	1.09, d (6.5)	1.22, d (6.6)	1.07, d (6.5)	1.06, d (6.6)	0.95, d (6.5)	0.96, d (6.5)	0.92, d (6.5)
2′	2.10, m	3.29	2.33, m	2.18, m	3.10, m	3.15, m	2.19, m
3′	1.69, m	2.20, m	1.93, m	1.82, m	2.15, m	1.94, m	1.87, m
	1.30, m	1.73, m	1.41, m	1.54, m	1.59, m	1.81, m	1.51, m
4′	1.58, m	2.00, m	1.60, m	1.61, m	1.81, m	1.90, m	1.63, m
	1.48, m					1.81, m	
5′	2.91, m	3.61, brs	2.92, m	2.87, m	3.28, m 2.67, m	3.34, m	2.95, m
	1.95, m	2.99, brs	2.07, q (8.9)	2.06, m		2.80, m	2.09, m
6′	1.81, m	2.13, m	1.88, m	1.73, m	1.92, m	1.93, m	1.68, m
	1.08, m	1.59, t (12.2)	1.23, m	1.56, m	1.49, m	1.82, m	1.59, m
7′	3.52, m	3.70, m	3.66, m	3.78, m	3.68, m	3.96, m	3.74, m
8′	1.17, d (6.1)	1.34, d (6.2)	1.20, d (6.3)	1.18, d (6.1)	1.21, d (6.2)	1.22, d (6.1)	1.16, d (6.2)
9′	2.15, s	2.86, s	2.20, s	2.22, s	2.52, s	2.68, s	2.24, s
2″		5.82, d (2.0)		5.72, s			5.72, s
3″	6.18, qd (7.3, 1.6)		6.08, qd (7.3, 1.6)		6.10, qd (7.2, 1.7)	6.12, qd (7.2, 1.7)	
4″	1.97, dq (7.3, 1.6)	1.96, d (2.0)	1.94, dq (7.3, 1.6)	1.88, s	1.93, dq (7.2, 1.7)	1.94, dq (7.2, 1.7)	1.89, s
5″	1.86, t (1.6)	2.21, d (2.0)	1.86, t (1.6)	2.10, s	1.86, t (1.7)	1.84, t (1.7)	2.10, s

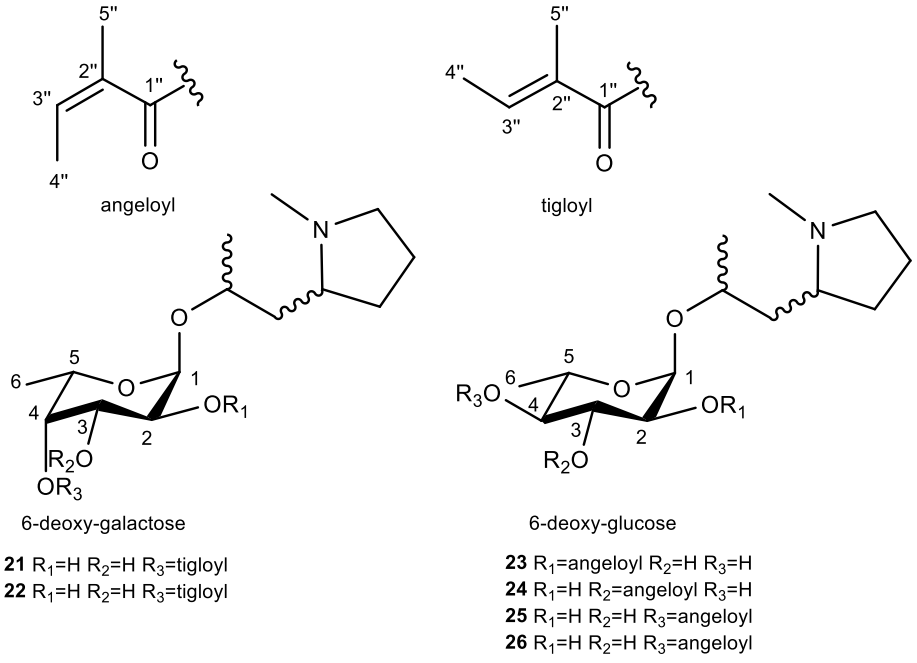

Fig. 6. Chemical structures of compounds **21**–**26**.

L. donovani and *P. falciparum*, which are the etiological agents of sleeping sickness, Chagas disease, visceral leishmaniasis and tropical malaria, respectively. The cytotoxicity in uninfected rat skeletal L6 cells was also evaluated. The data obtained are summarized in Table 7. A significant inhibiton (IC_{50} < 10 μg/mL) of the alkaloid extract was observed only towards *P. falciparum*. Among the isolated compounds, compounds **11**–**16** and **18** inhibited the etiologic agent of malaria with IC_{50} <10 μM. Thus the presence of two C_5 acids esterifying the sugar unit appears to be essential for the antiplasmodial activity because compounds with one C_5 acid only (compounds **4**, **6**–**10**) or without C_5 acid (compounds **1**–**3**) were inactive against the parasite (Table 7). The nature of the C_5 acid (angelic, senecioic or tiglic acid), their location on the sugar unit as well as the stereochemistry of the hygroline seemed to have a low influence on the antiplasmodial activity. In addition, the *trans*-cinnamoyl moiety esterified in C-4 for **18** was beneficial for the antiplasmodial activity (IC_{50} = 6.3 μM), whereas the *cis*-cinnamoyl moiety for **17** was detrimental (IC_{50} = 26.1 μM). No cytotoxicity was detected for all compounds.

3. Conclusions

The targeted investigation of pyrrolidine derivatives in the aerial parts of *S. tricolor* resulted in the isolation and characterization of 20 undescribed alkaloids named schizanthosides A1-A3 (**1**–**3**), B1–B7 (**4**–**10**), C1–C6 (**11**–**16**), D1-D2 (**17**–**18**), and E1-E2 (**19**–**20**). Six other pyrrolidine alkaloids were also isolated but not fully characterized due to lack of material. Compounds **11**–**16** and **18** showed a significant inhibitory activity towards *P. falciparum* with an IC_{50} < 10 μM.

Table 3
^{13}C NMR data of compounds **4**–**10** (150 MHz, in DMSO-d_6 or * CD_3OD, δ in ppm, C type).

Position	4	5*	6	7	8	9	10
1	97.2, CH	99.4, CH	100.0, CH	100.0, CH	100.6, CH	100.1, CH	99.9, CH
2	71.4, CH	72.4, CH	65.3, CH	65.4, CH	68.8, CH	68.3, CH	68.6, CH
3	66.9, CH	69.1, CH	73.5, CH	73.0, CH	67.4, CH	67.6, CH	68.0, CH
4	71.8, CH	73.7, CH	68.9, CH	69.2, CH	73.9, CH	73.8, CH	73.0, CH
5	66.0, CH	67.9, CH	65.8, CH	66.2, CH	64.8, CH	65.2, CH	64.9, CH
6	16.3, CH_3	16.4, CH_3	16.3, CH_3	16.3, CH_3	16.2, CH_3	16.3, CH_3	16.2, CH_3
2′	61.9, CH	67.4, CH	62.2, CH	63.8, CH	64.0, CH	65.5, CH	63.7, CH
3′	30.1 CH_2	30.3, CH_2	30.4, CH_2	28.7, CH_2	28.9, CH_2	27.3, CH_2	29.1, CH_2
4′	21.4, CH_2	22.2, CH_2	21.5, CH_2	21.2, CH_2	20.8, CH_2	20.7, CH_2	21.3, CH_2
5′	56.6, CH_2	57.1, CH_2	56.5, CH_2	56.2, CH_2	55.3, CH_2	55.2, CH_2	56.2, CH_2
6′	41.3, CH_2	39.0, CH_2	40.7, CH_2	37.5, CH_2	38.2, CH_2	34.6, CH_2	38.0, CH_2
7′	74.8, CH	75.9, CH	74.1, CH	73.7, CH	75.0, CH	74.1, CH	73.8, CH
8′	22.6, CH_3	22.5, CH_3	22.5, CH_3	21.9, CH_3	22.2, CH_3	21.7, CH_3	21.9, CH_3
9′	39.9, CH_3	39.4, CH_3	40.0, CH_3	39.6, CH_3	38.5, CH_3	38.1, CH_3	39.8, CH_3
1″	167.1, C	167.6, C	167.3, C	165.6, C	167.0, C	167.0, C	165.6, C
2″	127.3, C	116.5, CH	128.0, C	116.3, CH	127.8, C	127.7, C	116.0, CH
3″	138.7, CH	160.5, C	136.8, CH	155.9, C	136.8, CH	137.1, CH	156.3, C
4″	15.8, CH_3	27.5, CH_3	15.5, CH_3	26.8, CH_3	15.5, CH_3	15.6, CH_3	26.9, CH_3
5″	20.4, CH_3	20.5, CH_3	20.3, CH_3	19.9, CH_3	20.4, CH_3	20.5, CH_3	20.0, CH_3

Table 4
^{1}H NMR data of compounds **11**–**16** (600 MHz, in DMSO-d_6, δ in ppm, J in Hz).

Position	11	12	13	14	15	16
1	5.01, d (3.8)	5.00, d (3.9)	5.03, d (3.9)	4.85, d (3.9)	4.86, d (3.8)	4.91, d (3.9)
2	5.10, dd (11.0, 3.8)	4.76, dd (10.6, 3.8)	4.64, dd (10.5, 3.8)	3.79, dd (10.6, 3.8)	3.80, dd (10.6, 3.8)	3.70, dd (10.5, 3.8)
3	5.19, dd (11.0, 3.2)	4.09, dd (10.6, 3.6)	5.31, dd (10.5, 9.3)	5.06, dd (10.6, 3.5)	5.09, dd (10.6, 3.5)	5.11, dd (10.5, 3.5)
4	3.80, d (3.6)	5.21, d (3.6)	3.21, t (9.3)	5.24, d (3.5)	5.28, d (3.5)	5.26, dd (3.5, 1.3)
5	4.04, dd (6.5, 1.3)	4.17, q (6.5)	3.78, m	4.21, dd (6.4, 1.3)	4.21, m	4.23, dd (6.4, 1.3)
6	1.12, d (6.5)	0.98, d (6.5)	1.18, d (6.3)	1.00, d (6.6)	1.00, d (6.8)	1.11, d (6.5)
2′	2.06, m	2.08, m	2.06, m	2.33, m	2.33, d (9.9)	2.15, m
3′	1.68, m 1.30, m	1.69, m 1.29, m	1.66, m 1.29, m	1.95, m 1.40, m	1.95, m 1.42, m	1.83, m 1.54, m
4′	1.57, m 1.48, m	1.57, m 1.48, m	1.57, m 1.46, m	1.59, m	1.60, m	1.62, m
5′	2.87, m 1.90, m	2.89, m 1.93, m	2.86, m 1.88, m	2.91 m 2.06 m	2.91 m 2.09 m	2.85, m 2.01, d (9.0)
6′	1.85, m 1.09, m	1.84, m 1.09, m	1.87, m 1.10, m	1.89, m 1.25, m	1.90, m 1.25, m	1.76, m 1.58, m
7′	3.59, m	3.57, m	3.62, m	3.71, m	3.73, m	3.82, m
8′	1.22, d (6.1)	1.19, d (6.1)	1.23, d (6.2)	1.22, d (6.2)	1.23, d (6.1)	1.21, d (6.5)
9′	2.13, s	2.14, s	2.13, s	2.19, s	2.20, s	2.22, s
3″	6.19, qd (7.3, 1.9)	6.20, qd (7.3, 1.7)	6.21, qd (7.3, 1.7)	6.67, qd (7.2, 1.8)	6.08, q (7.2)	6.07, qd (7.2, 1.6)
4″	1.87, m	1.96, m	1.89, m	1.73, dd (7.0, 1.4)	1.87, m	1.86, m
5″	1.78, dt (8.9, 1.6)	1.87, dt (8.9, 1.6)	1.75, t (1.6)	1.70, t (1.4)	1.74, m	1.74, m
3‴	6.11, qd (7.2, 1.5)	6.14, qd (7.2, 1.5)	6.05, qd (7.2, 1.6)	6.16, qd (7.2, 1.6)	6.17, q (7.4)	6.17, qd (7.1, 1.7)
4‴	1.87, m	1.96, m	1.84, m	1.90, m	1.92, dd (7.4, 1.7)	1.92, d (7.3)
5‴	1.78, dt (8.9, 1.6)	1.87, dt (8.9, 1.6)	1.79, t (1.6)	1.86, t (1.6)	1.87, m	1.86, m

Table 5
^{13}C NMR data of compounds **11**–**16** (150 MHz, in DMSO-d_6, δ in ppm, C type).

Position	11	12	13	14	15	16
1	97.1, CH	97.2, CH	96.3, CH	99.5, CH	99.7, CH	100.2, CH
2	68.3, CH	71.4, CH	71.4, CH	65.9, CH	66.2, CH	66.8, CH
3	70.1, CH	64.7, CH	71.2, CH	70.3, CH	70.3, CH	71.2, CH
4	68.9, CH	74.0, CH	72.9, CH	70.6, CH	71.0, CH	71.5, CH
5	65.9, CH	64.5, CH	67.3, CH	63.8, CH	64.1, CH	64.9, CH
6	16.1, CH_3	16.1, CH_3	17.0, CH_3	15.6, CH_3	15.9, CH_3	16.4, CH_3
2′	61.8, CH	61.8, CH	61.5, CH	61.9, CH	62.2, CH	64.1, CH
3′	30.1, CH_2	30.1, CH_2	29.9, CH_2	30.1, CH_2	30.4, CH_2	29.2, CH_2
4′	21.4, CH_2	21.3, CH_2	21.1, CH_2	21.2, CH_2	21.5, CH_2	21.7, CH_2
5′	56.7, CH_2	56.6, CH_2	56.4, CH_2	56.2, CH_2	56.5, CH_2	56.7, CH_2
6′	41.4, CH_2	41.3, CH_2	41.3, CH_2	40.6, CH_2	40.7, CH_2	38.1, CH_2
7′	75.3, CH	75.3, CH	75.4, CH	74.4, CH	74.6, CH	74.6, CH
8′	22.7, CH_3	22.6, CH_3	22.5, CH_3	22.1, CH_3	22.4, CH_3	22.3, CH_3
9′	39.9, CH_3	39.9, CH_3	39.7, CH_3	39.9, CH_3	40.0, CH_3	40.2, CH_3
1″	166.5, C	166.8, C	165.9, C	166.1, C	166.5, C	167.0, C
2″	127.3, C	127.1, C	126.2, C	127.6, C	127.3, C	127.8, C
3″	139.5, CH	139.3, CH	139.9, CH	136.9, CH	137.8, CH	137.9, CH
4″	15.4, CH_3	15.6, CH_3	15.4, CH_3	13.9, CH_3	15.4, CH_3	15.8, CH_3
5″	20.1, CH_3	20.4, CH_3	19.8, CH_3	11.4, CH_3	19.9, CH_3	20.4, CH_3
1‴	166.6, C	166.9, C	166.3, C	166.3, C	166.6, C	167.1, C
2‴	126.7, C	127.6, C	127.2, C	126.8, C	127.0, C	127.5, C
3‴	137.8, CH	137.3, CH	136.4, CH	137.5, CH	138.2, CH	138.6, CH
4‴	15.6, CH_3	15.7, CH_3	15.1, CH_3	15.1, CH_3	15.5, CH_3	16.0, CH_3
5‴	20.2, CH_3	20.4, CH_3	20.0, CH_3	20.0, CH_3	20.3, CH_3	20.7, CH_3

4. Experimental

4.1. General experimental procedures

Optical rotations were measured on a JASCO P-1030 (Easton, MD, USA) polarimeter. VCD spectra were recorded on a Bruker PMA 50 accessory coupled to a Tensor 27 Fourier transform infrared spectrometer (Billerica, MA, USA). A photoelastic modulator (Hinds PEM 90,

Table 6
^{1}H and ^{13}C NMR data of compounds **17**–**20** (600 and 150 MHz, in DMSO-d_6, δ in ppm).

Position	17 δ_H, (*J* in Hz)	δ_C, type	18 δ_H, (*J* in Hz)	δ_C, type	19 δ_H, (*J* in Hz)	δ_C, type	20 δ_H, (*J* in Hz)	δ_C, type
1	4.72, d (3.9)	100.0, CH	4.78, d (3.8)	100.0, CH	5.04, d (3.8)	96.8, CH	5.06, d (3.9)	96.9, CH
2	3.48, dd (10.2, 3.9)	68.2, CH	3.64, dd (10.3, 3.8)	68.4, CH	4.98, dd (11.1, 3.8)	68.2, CH	5.00, dd (11.2, 3.9)	68.1, CH
3	3.76, dd (10.2, 3.6)	67.1, CH	3.78, dd (10.3, 3.7)	67.1, CH	5.19, dd (11.1, 3.2)	68.9, CH	5.27, dd (11.2, 3.2)	68.8, CH
4	5.11, d (3.6)	74.0, CH	5.16, d (3.7)	74.0, CH	4.01, d (3.2)	76.5, CH	4.03, d (3.2)	76.3, CH
5	4.08, q (6.6)	64.4, CH	4.11, q (6.6)	64.5, CH	4.06, q (6.6)	65.9, CH	4.08, q (6.6)	66.1, CH
6	0.96, d (6.6)	16.0, CH_3	0.97, d (6.6)	16.0, CH_3	1.14, d (6.6)	16.0, CH_3	1.15, d (6.6)	16.2, CH_3
2′	2.34, m	62.0, CH		62.1, CH	2.09, m	62.0, CH	2.01, m	61.8, CH
3′	1.95, m	30.0, CH_2	1.99, m	29.9, CH_2	1.66, m	29.7, CH_2	1.66, m	30.1, CH_2
	1.40, m		1.44, m		1.30, m		1.28, m	
4′	1.61, m	21.2, CH_2	1.65, m	21.2, CH_2	1.57, m	21.1, CH_2	1.55, m	21.4, CH_2
					1.45, m		1.46, m	
5′	2.92, m	56.2, CH_2	2.98, m	56.1, CH_2	2.92, m	56.2, CH_2	2.86, m	56.7, CH_2
	2.06, m		2.16, m		1.92, m		1.87, m	
6′	1.84, m	40.6, CH_2	1.87, m	40.3, CH_2	1.87, m	40.8, CH_2	1.85, m	41.5, CH_2
	1.20, m		1.26, m		1.13, m		1.07, ddd (12.8, 10.0, 2.6)	
7′	3.63, m	74.3, CH	3.65, m	74.3, CH	3.59, ddd (9.2, 6.2, 2.7)	75.2, CH	3.59, m	75.5, CH
8′	1.18, d (6.2)	22.3, CH_3	1.20, d (6.3)	22.1, CH_3	1.21, d (6.2)	22.3, CH_3	1.21, d (6.1)	22.6, CH_3
9′	2.19, s	39.7, CH_3	2.25, s	39.6, CH_3	2.15, s	39.6, CH_3	2.11, s	39.8, CH_3
1″		165.4, C		165.8, C		166.5, C		166.2, C
2″	6.06, d (12.8)	119.4, CH	6.66, d (16.0)	118.1, CH		127.6, C		126.3, C
3″	7.01, d (12.8)	141.9, CH	7.65, d (16.0)	144.2, CH	6.73, m	138.0, CH	6.25, qd (7.3, 1.6)	140.4, CH
4″		134.5, C		133.8, C	1.73, m	14.0, CH_3	1.90, dq (7.3, 1.6)	15.8, CH_3
5″	7.66, dd (7.4, 2.2)	129.6, CH	7.74, m	128.1, CH	1.71, m	11.6, CH_3	1.77, t (1.6)	20.2, CH_3
6″	7.35, m	128.9, CH	7.43, m	130.3, CH				
7″	7.35, m	127.8, CH	7.43, m	128.7, CH				
8″	7.35, m	128.9, CH	7.43, m	130.3, CH				
9″	7.66, dd (7.4, 2.2)	129.6, CH	7.74, m	128.1, CH				
1‴						166.5, C		166.5, C
2‴						127.6, C		126.8, C
3‴					6.73, m	138.0, CH	6.17, qd (7.3, 1.6)	139.2, CH
4‴					1.73, m	14.0, CH_3	1.85, dq (7.3, 1.6)	15.8, CH_3
5‴					1.71, m	11.6, CH_3	1.77, t (1.6)	20.2, CH_3
1⁗					4.57, d (1.7)	101.6, CH	4.59, d (1.8)	101.8, CH
2⁗					3.76, m	70.1, CH	3.76, m	70.3, CH
3⁗					3.48, dd (9.4, 5.6, 3.2)	70.1, CH	3.47, dd (9.4, 3.2)	70.4, CH
4⁗					3.17, td (9.4, 5.6)	71.4, CH	3.18, t (9.4)	71.7, CH
5⁗					3.65, m	68.9, CH	3.66, m	69.1, CH
6⁗					0.91, d (6.1)	17.5, CH_3	0.95, d (6.2)	18.0, CH_3

Table 7
Antitrypanosomatid, antiplasmodial and cytotoxic activities of compounds **1**–**4**, **6**–**18**.

Compound	*T. b. rhodesiense*	*T. cruzi*	*L. donovani*	*P. falciparum*	Cytotoxicity
	IC_{50} [μM]				
1	49.3	88.0	>100	>100	>100
2	80.9	>100	>100	>100	>100
3	>100	>100	>100	>100	>100
4	>100	>100	>100	>100	>100
6	>100	>100	>100	94.0	>100
7	>100	>100	>100	>100	>100
8	>100	>100	66.2	27.2	>100
9	>100	>100	>100	65.7	>100
10	>100	>100	68.9	>100	>100
11	25.7	>100	94.6	6.8	>100
12	23.7	>100	81.8	7.3	>100
13	21.2	>100	>100	6.3	>100
14	17.5	>100	>100	8.7	>100
15	11.6	>100	53.2	2.8	>100
16	13.1	>100	91.1	6.0	>100
17	94.5	>100	>100	26.1	>100
18	18.9	>100	>100	6.3	>100
Schizanthus extract [a]	31.8	65.0	59.6	8.9	>100
Melarsoprol [b]	0.013				
Benznidazole [b]		2.8			
Miltefosine [b]			0.55		
Chloroquine [b]				0.006	
Podophyllotoxin [b]					0.027

Results are the means of two independent assays.
[a] IC_{50} is expressed in μg/mL.
[b] Positive controls.

Hinds Instruments, Hillsboro, OR, USA) set at l/4 retardation was used to modulate the handedness of the circular polarized light. Demodulation was performed by a lock-in amplifier (SR830 DSP, Stanford Research System, Sunnyvale, CA, USA). An optical low-pass filter (<1800 cm^{-1}) in front of the photoelastic modulator was used to enhance the signal/noise ratio. Solutions of 2.5–4 mg in 170 μL of DMSO-d_6 were prepared and measured in a transmission cell equipped with CaF_2 windows and a 200 μm spacer. Artifacts were eliminated by subtracting the VCD spectrum of the pure solvent (reference) from the VCD spectrum of the compound. For both the sample and the reference, ca. 24,000 scans at 4 cm^{-1} resolution were averaged. UV spectra were recorded on a PerkinElmer Lambda-25 UV–vis spectrophotometer (Wellesley, MA, USA). IR spectra were measured on a PerkinElmer Spectrum 100 spectrometer. NMR spectra were recorded on a Bruker Avance III HD 600 MHz NMR spectrometer equipped with a QCI 5 mm Cryoprobe and a SampleJet automated sample changer (Bruker BioSpin, Rheinstetten, Germany). Chemical shifts are reported in parts per million (δ) using the residual CD_3OD signals (δ_H 3.31; δ_C 49.0) or DMSO-d_6 signal (δ_H 2.50; δ_C 39.5) as internal standards for ^1H and ^{13}C NMR, respectively. HRMS spectra were obtained on a Q Exactive Focus Hybrid quadripole-orbitrap mass spectrometer (Thermo Scientific, Waltham, MA, USA) using electrospray in the positive mode. The spray voltage was set to 3.5 kV; the sheath gas flow rate (N_2) to 50 units; the capillary temperature to 320 °C; the S lens RF level to 50; and the probe heater temperature to 425 °C. UHPLC was performed on an Acquity UPLC I-class System (Waters, Milford, MA, USA). The separation was performed on an Acquity BEH C_{18} UPLC column (150 × 2.1 mm i.d.; 1.7 μm, Waters), using a gradient (H_2O and MeCN both containing 0.1% formic acid) of 5–30% MeCN in 35 min, followed by a washing step with 98% MeCN for 2 min. After the washing step, the column was equilibrated with 5% MeCN for 5 min before the next injection. The flow rate was set to 0.4 mL/min, the temperature to 40 °C, and the injection volume was 1 μL. Flash chromatography was performed on an Armen Spot preparative chromatographic system (Interchim, Montluçon, France) equipped with a quaternary pump, a UV detector, and a fraction collector. Reverse phase semi-preparative chromatography was performed on an Armen Spot preparative chromatographic system with a Kinetex Axia Core Shell C_{18} column (250 × 21.2 mm; 5 μm, Phenomenex) or an X-Select CSH C_{18} column (250 × 19 mm, 5 μm; Waters). The flow rate was set to 20 and 18 mL/min, respectively, and UV absorbance was at 220 nm. The control of fractions was carried out by an Acquity UPLC System (Waters) equipped with an Acquity PDA detector and connected to a Quattro Micro triple quadrupole mass spectrometer (Waters) with an ESI source operating in positive mode.

4.2. NMR computational details

All calculations have been performed with the Gaussian 16 program (Frisch et al., 2016). Geometry optimization has been achieved using density function theory (DFT) with the B3LYP functional and the 6-31G (d) basis set in the gas-phase. Vibrational analysis was completed at the same level to confirm a minimum. NMR prediction was performed using the mPW1PW91/6–31 + g(d,p) level.

4.3. Plant material

The aerial parts of *Schizanthus tricolor* Grau & Gronbach (Solanaceae) were collected in December 2003 in Cachagua, Chile (GPS coordinates 32°59′S; 71°44′W). Their identification was confirmed by Prof. Fernanda Pérez (Departamento de Botanica, Universidad de Chile). A voucher specimen was deposited at the Facultad de Ciencas Quimicas (N° 2000-3).

4.4. Extraction and isolation

The plant material (1.3 kg) was extracted successively with hexane and MeOH at room temperature. After filtration, the alcoholic solution was evaporated to dryness. The residue (161.2 g) was taken up in 0.1 M HCl and extracted with Et_2O. The aqueous solution was basified with 4% NH_4OH to pH 12 and then extracted with CH_2Cl_2. The organic solvent was dried with anhydrous Na_2SO_4, filtered, and evaporated, yielding 3.7 g of a gummy alkaline residue. The residue was submitted to a fractionation using two flash columns connected in series (PF–C_{18}HQ/120 g, 15 μm C_{18}, Interchim) with a gradient of 5–40% MeCN + 0.1% FA in 2 h and afforded 35 fractions. Fractions 1 and 2 were grouped (91.5 mg) and fractionated with the Kinetex column using a gradient of 0–15% MeOH + 0.1% NH_4OH in 90 min, and yielded **1** (15.1 mg), **2** (6.0 mg), and **3** (2.5 mg). Fraction 3 (23.9 mg) was separated with the Kinetex column using a gradient of 5–20% MeOH + 0.1% NH_4OH in 60 min and afforded **4** (2.3 mg) and **21** (0.3 mg). Fraction 4 (40.8 mg) was separated with the X-Select column using a gradient of 5–25% MeOH + 0.1% NH_4OH in 60 min and gave **5** (0.7 mg), **6** (1.4 mg), **7** (1.0 mg) and **22** (0.3 mg). Fraction 5 (28.4 mg) was separated with the Kinetex column using a gradient of 10–30% MeOH + 0.1% NH_4OH in 60 min and afforded **8** (3.0 mg), **23** (0.2 mg) and **24** (0.3 mg). Fraction 6 (40.3 mg) was separated with the Kinetex column using a gradient of 10–30% ACN in 60 min and afforded **9** (2.6 mg), **25** (0.2 mg) and **26** (0.2 mg). Fraction 7 (35.4 mg) was separated with the Kinetex column using a gradient of 15–35% MeOH + 0.1% NH_4OH in 60 min and gave **10** (1.0 mg) and **17** (0.9 mg). Fraction 8 (30.4 mg) was separated with the Kinetex column using a gradient of 15–40% MeOH + 0.1% NH_4OH in 60 min and gave **19** (0.5 mg). Fraction 10 (20.8 mg) was separated with the X-Select column using a gradient of 15–40% MeOH + 0.1% NH_4OH in 60 min and gave **20** (0.9 mg). Fraction 11 (25.9 mg) was separated with the Kinetex column using a gradient of 15–45% MeOH + 0.1% NH_4OH in 60 min and gave **18** (1.3 mg). Fractions 12 and 13 were grouped (45.8 mg) and fractionated with the Kinetex column using a gradient of 15–40% ACN in 60 min and yielded **11** (3.8 mg). Fraction 15 (16.6 mg) was separated with the Kinetex column using a gradient of 20–45% MeOH + 0.1% NH_4OH in 60 min and afforded **12** (4.0 mg). Fraction 18 (40.6 mg) was separated with the Kinetex column using a gradient of 20–45% MeOH + 0.1% NH_4OH in 60 min and gave **13** (1.6 mg). Fraction 22 (32.0 mg) was separated with the X-Select column using a gradient of 25–50% MeOH + 0.1% NH_4OH in 60 min and gave **14** (1.1 mg). Fraction 25 (28.0 mg) was separated with the X-Select column using a gradient of 30–55% MeOH + 0.1% NH_4OH in 60 min and gave **15** (3.8 mg). Fraction 30 (25.0 mg) was separated with the X-Select column using a gradient of 30–55% MeOH + 0.1% NH_4OH in 60 min and gave **16** (2.5 mg).

4.4.1. Schizanthoside A1 (1)

Pale yellow oil; $[\alpha]_D^{22}$ - 33.2 (*c* 0.05, MeOH); UV (MeOH) λ_{max} 222 nm; IR (neat) ν_{max} 3255, 2907, 1592, 1458, 1377, 1342 cm^{-1}; ^1H and ^{13}C NMR, see Table 1; HRESIMS *m/z* 290.1979 $[M + H]^+$ (calcd for $C_{14}H_{27}NO_5$, 290.1962).

4.4.2. Schizanthoside A2 (2)

Pale yellow oil; $[\alpha]_D^{22}$ - 56.7 (*c* 0.05, MeOH); UV (MeOH) λ_{max} 222 nm; IR (neat) ν_{max} 3305, 2923, 1596, 1452, 1345, 1050 cm^{-1}; ^1H and ^{13}C NMR, see Table 1; HRESIMS *m/z* 290.1979 $[M + H]^+$ (calcd for $C_{14}H_{27}NO_5$, 290.1962).

4.4.3. Schizanthoside A3 (3)

Pale yellow oil; $[\alpha]_D^{22}$ - 40.3 (*c* 0.07, MeOH); UV (MeOH) λ_{max} 222 nm; IR (neat) ν_{max} 3293, 2912, 1593, 1455, 1375, 1345 cm^{-1}; ^1H and ^{13}C NMR, see Table 1; HRESIMS *m/z* 290.1979 $[M + H]^+$ (calcd for $C_{14}H_{27}NO_5$, 290.1962).

4.4.4. Schizanthoside B1 (4)

Pale yellow oil; $[\alpha]_D^{22}$ - 78.6 (*c* 0.07, MeOH); UV (MeOH) λ_{max} 220 nm; IR (neat) ν_{max} 3325, 2934, 1711, 1599, 1457, 1376 cm^{-1}; ^1H and ^{13}C

NMR, see Tables 2 and 3; HRESIMS *m/z* 372.2385 $[M + H]^+$ (calcd for $C_{19}H_{34}NO_6$, 372.2381).

4.4.5. Schizanthoside B2 (5)

Pale yellow oil; $[\alpha]_D^{22}$ and IR not measured due to lack of material; UV (MeOH) λ_{max} 220 nm; ^{1}H and ^{13}C NMR, see Tables 2 and 3; HRESIMS *m/z* 372.2385 $[M + H]^+$ (calcd for $C_{19}H_{34}NO_6$, 372.2381).

4.4.6. Schizanthoside B3 (6)

Pale yellow oil; $[\alpha]_D^{22}$ - 71.6 (*c* 0.05, MeOH); UV (MeOH) λ_{max} 220 nm; IR (neat) ν_{max} 3351, 2929, 1706, 1595, 1457, 1353 cm^{-1}; ^{1}H and ^{13}C NMR, see Tables 2 and 3; HRESIMS *m/z* 372.2385 $[M + H]^+$ (calcd for $C_{19}H_{34}NO_6$, 372.2381).

4.4.7. Schizanthoside B4 (7)

Pale yellow oil; $[\alpha]_D^{22}$ - 81.0 (*c* 0.05, MeOH); UV (MeOH) λ_{max} 220 nm; IR (neat) ν_{max} 3352, 2970, 2927, 1714, 1650, 1599, 1449, 1142, 1082, 1043 cm^{-1}; ^{1}H and ^{13}C NMR, see Tables 2 and 3; HRESIMS *m/z* 372.2385 $[M + H]^+$ (calcd for $C_{19}H_{34}NO_6$, 372.2381).

4.4.8. Schizanthoside B5 (8)

Pale yellow oil; $[\alpha]_D^{22}$ - 62.7 (*c* 0.05, MeOH); UV (MeOH) λ_{max} 220 nm; IR (neat) ν_{max} 3360, 2936, 1713, 1597, 1457, 1352 cm^{-1}; ^{1}H and ^{13}C NMR, see Tables 2 and 3; HRESIMS *m/z* 372.2385 $[M + H]^+$ (calcd for $C_{19}H_{34}NO_6$, 372.2381).

4.4.9. Schizanthoside B6 (9)

Pale yellow oil; $[\alpha]_D^{22}$ - 72.2 (*c* 0.05, MeOH); UV (MeOH) λ_{max} 220 nm; IR (neat) ν_{max} 3344, 2927, 1712, 1597, 1453, 1380 cm^{-1}; ^{1}H and ^{13}C NMR, see Tables 2 and 3; HRESIMS *m/z* 372.2385 $[M + H]^+$ (calcd for $C_{19}H_{34}NO_6$, 372.2381).

4.4.10. Schizanthoside B7 (10)

Pale yellow oil; $[\alpha]_D^{22}$ - 91.8 (*c* 0.05, MeOH); UV (MeOH) λ_{max} 220 nm; IR (neat) ν_{max} 3307, 2935, 1706, 1650, 1597, 1449, 1026 cm^{-1}; ^{1}H and ^{13}C NMR, see Tables 2 and 3; HRESIMS *m/z* 372.2385 $[M + H]^+$ (calcd for $C_{19}H_{34}NO_6$, 372.2381).

4.4.11. Schizanthoside C1 (11)

Pale yellow oil; $[\alpha]_D^{22}$ - 65.1 (*c* 0.07, MeOH); UV (MeOH) λ_{max} 221 nm; IR (neat) ν_{max} 3376, 2934, 1713, 1600, 1457, 1354 cm^{-1}; ^{1}H and ^{13}C NMR, see Tables 4 and 5; HRESIMS *m/z* 454.2797 $[M + H]^+$ (calcd for $C_{24}H_{40}NO_7$, 454.2800).

4.4.12. Schizanthoside C2 (12)

Pale yellow oil; $[\alpha]_D^{22}$ - 65.4 (*c* 0.07, MeOH); UV (MeOH) λ_{max} 221 nm; IR (neat) ν_{max} 3341, 2934, 1713, 1602, 1457, 1356 cm^{-1}; ^{1}H and ^{13}C NMR, see Tables 4 and 5; HRESIMS *m/z* 454.2797 $[M + H]^+$ (calcd for $C_{24}H_{40}NO_7$, 454.2800).

4.4.13. Schizanthoside C3 (13)

Pale yellow oil; $[\alpha]_D^{22}$ - 32.2 (*c* 0.05, MeOH); UV (MeOH) λ_{max} 221 nm; IR (neat) ν_{max} 3351, 2970, 1723, 1602, 1449, 1367 cm^{-1}; ^{1}H and ^{13}C NMR, see Tables 4 and 5; HRESIMS *m/z* 454.2797 $[M + H]^+$ (calcd for $C_{24}H_{40}NO_7$, 454.2800).

4.4.14. Schizanthoside C4 (14)

Pale yellow oil; $[\alpha]_D^{22}$ - 46.7 (*c* 0.05, MeOH); UV (MeOH) λ_{max} 221 nm; IR (neat) ν_{max} 3351, 2927, 1713, 1596, 1453, 1037 cm^{-1}; ^{1}H and ^{13}C NMR, see Tables 4 and 5; HRESIMS *m/z* 454.2797 $[M + H]^+$ (calcd for $C_{24}H_{40}NO_7$, 454.2800).

4.4.15. Schizanthoside C5 (15)

Pale yellow oil; $[\alpha]_D^{22}$ - 46.5 (*c* 0.07, MeOH); UV (MeOH) λ_{max} 221 nm; IR (neat) ν_{max} 3353, 2935, 1719, 1595, 1456, 1377 cm^{-1}; ^{1}H and ^{13}C NMR, see Tables 4 and 5; HRESIMS *m/z* 454.2797 $[M + H]^+$ (calcd for $C_{24}H_{40}NO_7$, 454.2800).

4.4.16. Schizanthoside C6 (16)

Pale yellow oil; $[\alpha]_D^{22}$ - 45.7 (*c* 0.07, MeOH); UV (MeOH) λ_{max} 221 nm; IR (neat) ν_{max} 3353, 2970, 1739, 1456, 1368 cm^{-1}; ^{1}H and ^{13}C NMR, see Tables 4 and 5; HRESIMS *m/z* 454.2797 $[M + H]^+$ (calcd for $C_{24}H_{40}NO_7$, 454.2800).

4.4.17. Schizanthoside D1 (17)

Pale yellow oil; $[\alpha]_D^{22}$ - 43.2 (*c* 0.05, MeOH); UV (MeOH) λ_{max} 221, 282 nm; IR (neat) ν_{max} 3327, 2940, 2831, 1709, 1601, 1450, 1023 cm^{-1}; ^{1}H and ^{13}C NMR, see Table 6; HRESIMS *m/z* 420.2388 $[M + H]^+$ (calcd for $C_{23}H_{34}NO_6$, 420.2381).

4.4.18. Schizanthoside D2 (18)

Pale yellow oil; $[\alpha]_D^{22}$ - 74.3 (*c* 0.05, MeOH); UV (MeOH) λ_{max} 220, 282 nm; IR (neat) ν_{max} 3350, 2939, 2830, 1715, 1597, 1450, 1024 cm^{-1}; ^{1}H and ^{13}C NMR, see Table 6; HRESIMS *m/z* 420.2388 $[M + H]^+$ (calcd for $C_{23}H_{34}NO_6$, 420.2381).

4.4.19. Schizanthoside E1 (19)

Pale yellow oil; $[\alpha]_D^{22}$ not measured due to lack of material; UV (MeOH) λ_{max} 221 nm; IR (neat) ν_{max} 3349, 2930, 1711, 1597, 1454, 1024 cm^{-1}; ^{1}H and ^{13}C NMR, see Table 6; HRESIMS *m/z* 600.3386 $[M + H]^+$ (calcd for $C_{30}H_{50}NO_{11}$, 600.3379).

4.4.20. Schizanthoside E2 (20)

Pale yellow oil; $[\alpha]_D^{22}$ not measured due to lack of material; UV (MeOH) λ_{max} 221 nm; IR (neat) ν_{max} 3351, 2937, 1708, 1596, 1452, 1024 cm^{-1}; ^{1}H and ^{13}C NMR, see Table 6; HRESIMS *m/z* 600.3386 $[M + H]^+$ (calcd for $C_{30}H_{50}NO_{11}$, 600.3379).

4.5. Acid hydrolysis of 1 and 2

A solution of **1** and **2** (3.0 mg each, individually) in 10% HCl (2 mL) was heated for 3 h. Then, the solution was basified with NaOH (2 M) until pH 12, and then extracted with CH_2Cl_2 (3 × 4 mL). (−)-Hygroline and (+)-pseudohygroline were confirmed by comparison of their optical rotation with the literature (Liniger et al., 2013) or by comparison with a reference sample for the L-fucose; $[\alpha]_D^{20}$ -75.5 (*c* 4, H_2O).

4.6. Antitrypanosomal, antileishmanial, antiplasmodial, and cytotoxicity assays

The in vitro activity against *T. b. rhodesiense*, *T. cruzi*, *L. donovani and P. falciparum* as well as cytotoxicity assessment in L6 cells were determined as reported elsewhere (Bernal et al., 2020). The strains were *T. b. rhodesiense* STIB 900 bloodstream form (trypomastigote), *T. cruzi* Tulahuen C2C4 (LacZ) amastigote form grown in rat L6 skeletal myoblasts, *L. donovani* MHOM/ET/67/L82 amastigote form, and *P. falciparum* NF54 erythrocytic stage. Results are expressed in μM for pure compounds.

Declaration of competing interest

The authors declare that they have no known competing financial interests or personal relationships that could have appeared to influence the work reported in this paper.

Acknowledgments

We thank Romina Rocchetti, Sonja Märki and Monical Cal for expert technical assistance in drug testing. This work was supported by the

Swiss National Science Foundation (SNF grant CRSII5_183536). The Institute of Pharmaceutical Sciences of Western Switzerland is thankful to the Swiss National Science Foundation for the support in the acquisition of the NMR 600 MHz (SNF R'Equip grant 316030_164095).

Appendix A. Supplementary data

Supplementary data to this article can be found online at https://doi.org/10.1016/j.phytochem.2021.112957.

References

Bernal, F.A., Kaiser, M., Wünsch, B., Schmidt, T.J., 2020. Structure−Activity relationships of cinnamate ester analogues as potent antiprotozoal agents. ChemMedChem 15, 68–78. https://doi.org/10.1002/cmdc.201900544.

Bhat, C., Tilve, S.G., 2011. Synthesis of (-)-hygrine, (-)-norhygrine, (-)-pseudohygroline and (-)-hygroline via nef reaction. Tetrahedron Lett. 52, 6566–6568. https://doi.org/10.1016/j.tetlet.2011.09.118.

Christen, P., Cretton, S., Humam, M., Bieri, S., Munoz, O., Joseph-Nathan, P., 2020. Chemistry and biological activity of alkaloids from the genus Schizanthus. Phytochemistry Rev. 19, 615–641. https://doi.org/10.1007/s11101-018-9598-5.

Cretton, S., Bartholomeusz, T.A., Mehl, F., Allenbach, Y., Matheeussen, A., Cos, P., Maes, L., Christen, P., 2014a. Synthesis and in vitro evaluation of tropane halogenated-derivatives against malaria, sleeping sickness, Chagas disease and leishmaniasis. Med. Chem. 10, 753–758. https://doi.org/10.2174/1573406410666140507095430.

Cretton, S., Breant, L., Pourrez, L., Ambuehl, C., Marcourt, L., Ebrahimi, S.N., Hamburger, M., Perozzo, R., Karimou, S., Kaiser, M., Cuendet, M., Christen, P., 2014b. Antitrypanosomal quinoline alkaloids from the roots of waltheria indica. J. Nat. Prod. 77, 2304–2311. https://doi.org/10.1021/np5006554.

Cretton, S., Glauser, G., Jeannerat, D., Munoz, O., Maes, L., Christen, P., Hostettmann, K., 2010. Isomeric tropane alkaloids from the aerial parts of Schizanthus tricolor. J. Nat. Prod. 73, 844–847. https://doi.org/10.1021/np900780w.

Cretton, S., Kaiser, M., Karimou, S., Ebrahimi, S.N., Maser, P., Cuendet, M., Christen, P., 2020. Pyridine-4(1H)-one alkaloids from waltheria indica as antitrypanosomatid agents. J. Nat. Prod. 83, 3363–3371. https://doi.org/10.1021/acs.jnatprod.0c00671.

De la Fuente, G., Reina, M., Muñoz, O., San Martin, A., Girault, J.P., 1988. Tropane alkaloids from Schizanthus pinnatus. Heterocycles 27, 1887–1897. https://doi.org/10.3987/COM-88-4562.

Frisch, M.J., Trucks, G.W., Schlegel, H.B., Scuseria, G.E., Robb, M.A., Cheeseman, J.R., Scalmani, G., Barone, V., Petersson, G.A., Nakatsuji, H., Li, X., Caricato, M., Marenich, A.V., Bloino, J., Janesko, B.G., Gomperts, R., Mennucci, B., Hratchian, H. P., Ortiz, J.V., Izmaylov, A.F., Sonnenberg, J.L., Williams, Ding F., Lipparini, F., Egidi, F., Goings, J., Peng, B., Petrone, A., Henderson, T., Ranasinghe, D., Zakrzewski, V.G., Gao, J., Rega, N., Zheng, G., Liang, W., Hada, M., Ehara, M., Toyota, K., Fukuda, R., Hasegawa, J., Ishida, M., Nakajima, T., Honda, Y., Kitao, O., Nakai, H., Vreven, T., Throssell, K., Montgomery Jr., J.A., Peralta, J.E., Ogliaro, F., Bearpark, M.J., Heyd, J.J., Brothers, E.N., Kudin, K.N., Staroverov, V.N., Keith, T.A., Kobayashi, R., Normand, J., Raghavachari, K., Rendell, A.P., Burant, J.C., Iyengar, S. S., Tomasi, J., Cossi, M., Millam, J.M., Klene, M., Adamo, C., Cammi, R., Ochterski, J. W., Martin, R.L., Morokuma, K., Farkas, O., Foresman, J.B., Fox, D.J., 2016. Gaussian 16. Rev. C.01, Wallingford, CT.

Islam, M.T., Mubarak, M.S., 2020. Pyrrolidine alkaloids and their promises in pharmacotherapy. Adv. Tradit. Med. 20, 13–22. https://doi.org/10.1007/s13596-019-00419-4.

Liniger, M., Estermann, K., Altmann, K.-H., 2013. Total synthesis of hygrolines and pseudohygrolines. J. Org. Chem. 78, 11066–11070. https://doi.org/10.1021/jo4017343.

Muñoz, O., Schneider, C., Breitmaier, E., 1994. A new pyrrolidine alkaloid from Schizanthus integrifolius. Liebigs Ann. Chem. 521–522. https://doi.org/10.1002/jlac.15619940513.

Pérez, F., Arroyo, M.T.K., Medel, R., Hershkovitz, M.A., 2006. Ancestral reconstruction of flower morphology and pollination systems in Schizanthus (Solanaceae). Am. J. Bot. 93, 1029–1038. https://doi.org/10.3732/ajb.93.7.1029.

Smith, S.G., Goodman, J.M., 2010. Assigning stereochemistry to single diastereoisomers by GIAO NMR calculation: the DP4 probability. J. Am. Chem. Soc. 132, 12946–12959. https://doi.org/10.1021/ja105035r.

Taniguchi, T., Monde, K., 2007a. Chiroptical analysis of glycoconjugates by vibrational circular dichroism (VCD). Trends Glycosci. Glycotechnol. 19, 147–164. https://doi.org/10.4052/tigg.19.147.

Taniguchi, T., Monde, K., 2007b. Spectrum-structure relationship in carbohydrate vibrational circular dichroism and its application to glycoconjugates. Chem. Asian J. 2, 1258–1266. https://doi.org/10.1002/asia.200700180.